Higher power density limit at COMD in GaInP/AlGaInP in quantum dots than in wells.

Stella. N. Elliott[*a], Peter. M. Smowton[a], Gareth T. Edwards[a], Graham Berry[b] Andrey B. Krysa[c]
[a]School of Physics and Astronomy, Cardiff University, Queens Buildings, The Parade, Cardiff, CF24 3AA U. K.
[b]IQE (Europe) Ltd, Cypress Drive, St Mellons, Cardiff CF3 0EG, UK
[c]EPSRC Central Facility for III-V Semiconductors, Dept. of Electronic and Electrical Engineering, University of Sheffield, Sheffield, S1 3YD, UK

ABSTRACT

Quantum dots (QD) offer significant advantages over quantum wells (QW) as the active material in high power lasers. We have determined power density values at catastrophic optical mirror damage (COMD), a key factor limiting high power laser diode performance, for various QW and QD red and NIR emitting structures in the in the AlGaInP system. The devices used were 50 μm oxide stripe lasers mounted p-side up on copper heatsinks operated pulsed. The COMD power density limit decreases as pulse length increases. At short pulse lengths the limit is higher in QD (19.1±1.1 MW/cm^2) than in QW devices (11.9±2.8 MW/cm^2 and 14.3±0.4 MW/cm^2 for two different spot sizes). We used the high energy Boltzmann tail of the spontaneous emission from the front facet to measure temperature rise to investigate the physical mechanisms (non-radiative recombination of injected carriers and reabsorption of laser light at the facet) leading to COMD and distinguish between the behaviour at COMD of QW and QD devices. Over the range 1x to 2x threshold current the temperature rise in the QW structures was higher. Scanning electron microscopy showed a difference between the QD and QW lasers in the appearance of the damage after COMD.

Keywords: COMD, AlGaInP, quantum dot, power density, spontaneous emission, facet, non-radiative recombination, reabsorption, SEM

1. INTRODUCTION

There is demand for high power single emitter red-emitting semiconductor lasers: uses are found in DVD RW applications (where backwards compatible capability is being built into Bluray systems), various medical applications such as photodynamic therapy [1], pump lasers and projection applications where high power, good energy conversion efficiency and good beam quality are required. The spot size of the beam at the facet (d/Γ where d is the well width and Γ is the confinement factor) can have an effect on the likelihood of Catastrophic Optical Mirror Damage (COMD). COMD occurs when heating occurs locally at the facet causing a temperature spiral which results in local melting and destruction of the laser facet with a partial or complete, irreversible drop in output laser power. It is a key factor limiting high power operation of laser diodes. The facet damage occurs at a critical power density which varies with the material system used: in the GaInP/AlGaInP system values as low as 3.5 MW/cm^2 [2] cw are seen.

The phenomenon of COMD has been and continues to be extensively studied. Early workers examined the defects created at and propagating from the heated facet regions and proposed models to explain the COMD temperature spiral. Henry suggested absorption of the laser light generated electron-hole pairs which then undergo non-radiative recombination causing heating of the facet and bandgap reduction followed by further absorption [3]. Chen and Tien suggested non radiative recombination of carriers at the facet causing heating, bandgap reduction and absorption in the cladding layer [4] as the starting point. Tang suggested a critical facet temperature had to be reached for the destructive spiral to take place [5]. Any defects at the facet act as centres for absorption and non-radiative recombination: dangling

[*] spxse@cf.ac.uk; phone +44 (0)29 208 75316; fax +44 (0)29 208 74056

Novel In-Plane Semiconductor Lasers VIII, edited by Alexey A. Belyanin, Peter M. Smowton,
Proc. of SPIE Vol. 7230, 72300X · © 2009 SPIE · CCC code: 0277-786X/09/$18 · doi: 10.1117/12.809341

bonds are left when any surface is produced by cleaving in addition to damage such as crystalline defects or oxidation caused when a laser with as-cleaved facets is operated.

Many processes exist to prevent or reduce the likelihood of COMD [6]. Facets can be passivated to reduce non-radiative recombination due to dangling bonds and coated to prevent oxidation. Current blocking layers can be used to prevent injected carriers migrating to the facet and recombining non-radiatively. Non-absorbing mirrors can be created by disordering of the quantum wells thus increasing the bandgap. These extra processing steps increase manufacturing costs and tend to increase the power density leading to COMD rather than preventing it completely. Use of a quantum dot (QD) as opposed to a QW active region could make such extra manufacturing steps unnecessary due to the different physical properties of QD active regions or increase the COMD limit still further. In addition quantum dots offer significant advantages as the active material in high power lasers, having threshold current density that is both low and insensitive to temperature and routinely low values of modal loss (α_i) enabling long lasers to be used.

Among the physical parameters that are advantageous in QD material is the surface recombination velocity: a parameter which quantifies the rate of in-plane carrier diffusion and thus directly affects the rate of non-radiative recombination and heating at the facet. It has been established that this is reduced by an order of magnitude in quantum dot lasers [7] at 980/1280 nm in the GaInAs system. In addition reduced filamentation has been observed in QD as compared to QW lasers [8 9] leading to a uniform distribution of power at the facet with no hot spots to seed COMD as well as higher optical beam quality.

We investigated these potential advantages with a number of experiments comparing the COMD limit for QW lasers of different spot size, QW with QD, QW as a function of pulse length, and also made some comparisons with different aluminium fractions in the cladding layers. All the devices emitted in the red/NIR region and were fabricated in the InP/GaInP/AlGaInP material system. We then made measurements of facet temperature rise in order to further investigate the differences observed between QW and QD.

2. DETERMINATION OF COMD POWER DENSITY VALUES

2.1 Structure and COMD power density values for QW structures

The QW structures used were commercial DVD laser designs chosen for their very different spot sizes: 0.541 µm and 0.373 µm although both had the same narrow farfield of about 18° FWHM [10]. The active regions of both structures consisted of three 5 nm compressively strained GaInP QWs separated by 5.5 nm $(Al_{0.5}Ga_{0.5})InP$ (lattice matched) barriers in $(Al_{0.7}Ga_{0.3})InP$ waveguides. (Figure 1). Both structures emitted at about 660nm.

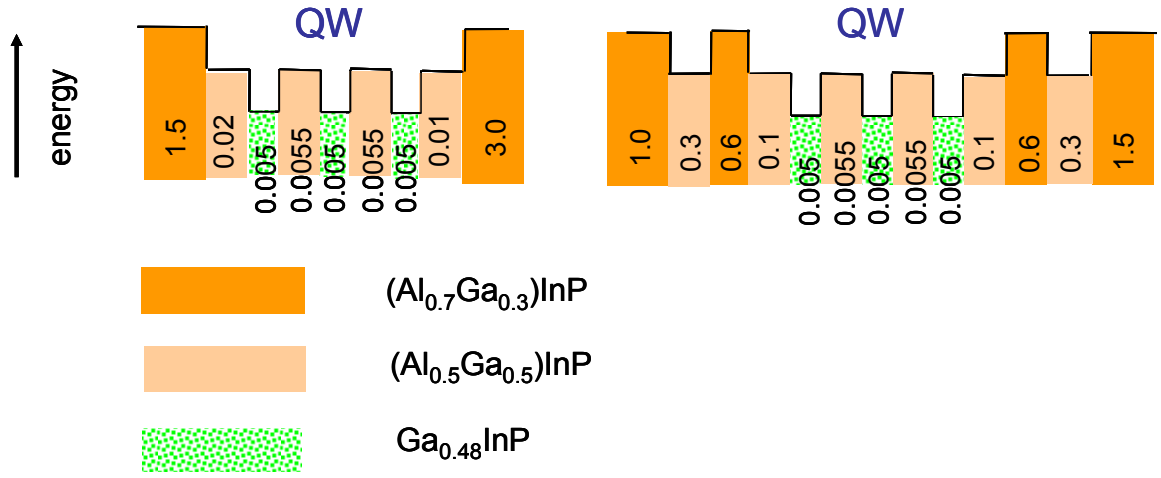

Figure 1 Structure of QW devices used in COMD experiments. Both structures have three compressively strained GaInP QW with AlGaInP waveguides and barriers. Dimensions shown on the diagram are in µm. The left hand structure has a spot size of 0.541µm and the right hand one has a spot size of 0.373 µm. Both structures operate at wavelengths of about 660 nm.

Sets of about ten 50 μm wide oxide isolated stripe lasers were prepared for the COMD measurements with as cleaved facets, mounted p-side up on copper heatsinks using conductive epoxy. The devices were operated pulsed (between 400 ns and 1000 ns at a repetition rate of 1 kHz) in order to ensure we were testing the intrinsic laser properties and not the effects of heating.

For the COMD experiment we first measured the nearfields of the devices which were then placed in an integrating sphere where the average optical power over the cycle was measured as a function of current. Using the known values of the duty cycle the peak optical power could be calculated. The COMD limit was determined when the optical power dropped abruptly to a small fraction of its previous value. The shapes of the P-I characteristics were checked to ensure COMD and not merely thermal rollover had taken place. The appearance of the facets was examined with optical and scanning electron microscopy (SEM) and damage typical of COMD was observed. (Figure 2) The beam area intersecting the facet was obtained by multiplying the FWHM nearfield by the calculated spot size and used with the peak power to obtain the power density at the facet. The group of three or so devices with the highest values was averaged to give the COMD value for that structure.

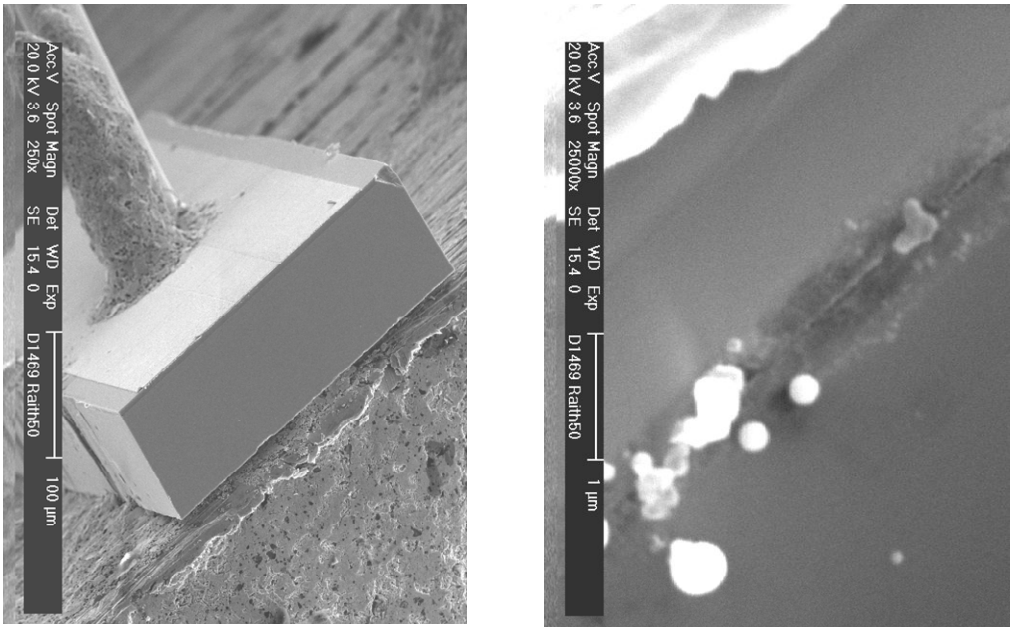

Figure 2 SEM pictures of a device that had undergone COMD. The whole of the facet is seen in the left hand diagram (the scale is given on the micrograph – 100 μm). A higher magnification picture of the same device is shown on the right hand (scale of 1 μm) showing the molten spheres extruded as COMD took place.

The peak powers obtained at COMD were 11.9 (± 2.8) MW/cm^2 for the large spot size structure and 14.3 (± 0.4) MW/cm^2 for the small. (Table 1). The errors here were taken as the maximum deviation from the mean value. Taking into account the experimental uncertainty the COMD power density limit was the same for both spot sizes.

2.2 COMD power density as a function of pulse length

It is known that pulse length affects the COMD limit [11] . If the length of the pulse is short any heat generated in the facet has time to dissipate before the next pulse. The heat from longer pulses or cw pumping causes a larger facet temperature rise due to the finite thermal conductivity of the epitaxial layers in the structure in addition to bulk joule heating. As the heat builds up in the device a critical facet temperature [12] is reached beyond which COMD proceeds very rapidly. A simple 1-d analytical model [13], assuming a monolithic block of material, predicts $1/t^{1/2}$ dependence of the temperature rise at the facet, where t is the pulse length. The results obtained in practice for a three dimensional multilayered structure show a similar trend. (Figure 3). It was thus necessary to carefully control the pulse length when comparing different structures.

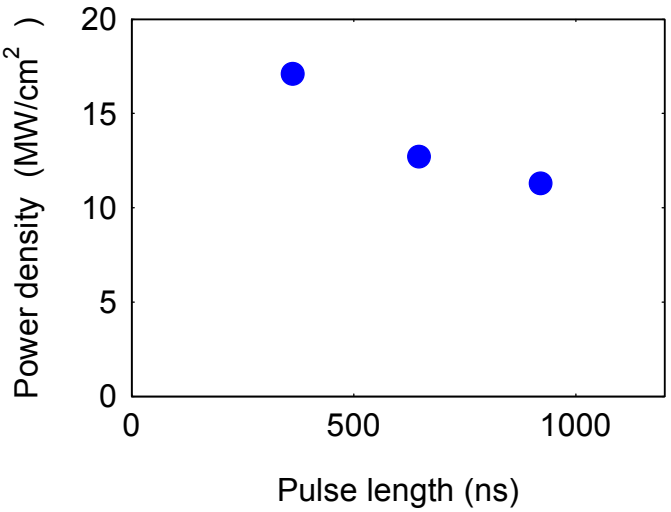

Figure 3 The COMD power density limit as a function of pulse length for a QW structure (small spot size QW)

2.3 Comparison of COMD power density values for QW and QD structures

The QW structures were then compared with a QD structure operated under the same conditions (400ns pulse length at 1 kHz). The QD structure, illustrated in Figure 4, consists of 5 layers of InP self assembled quantum dots in 8 nm GaInP quantum wells separated by 16 nm AlGaInP spacer layers, in AlInP cladding layers. These structures, which are still under development, were designed with a high confinement factor resulting in a small spot size of 0.251 µm. The COMD limit obtained was 19.1 (± 1.1) MW/cm^2 : outside the uncertainty limits of the measurements for the QW structures and thus significantly higher than the limit for both QW structures. (Table 1).

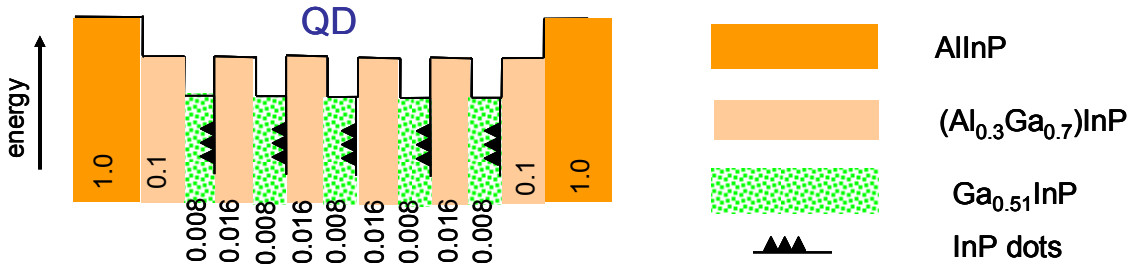

Figure 4 Comparison QD structure consisting of 5 layers of InP self assembled quantum dots in 8 nm GaInP quantum wells separated by 16 nm AlGaInP spacer layers, in AlInP cladding layers. Dimensions on the figure are in µm. The structure emitted at about 715 nm.

Table 1 showing COMD limit and spot size for two QW and one QD structures (operated at 400 ns pulse length 1 kHz repetition rate)

	Spot size (µm)	COMD power density MW/cm^2)
QW large spot size	0.541	11.9 (± 2.8)
QW small spot size	0.373	14.3 (± 0.4)
QD	0.251	19.1 (± 1.1)

Results for the COMD power density limit were obtained for a variety of structures looking at different spot sizes, pulse lengths, Al fractions in the cladding layers and different width spacer layers in the QD structures, some of which were p-doped. None of the factors investigated substantially affected the COMD limit apart from the pulse length and the QD/QW nature of the active region at short pulse lengths. (Figure 5.)

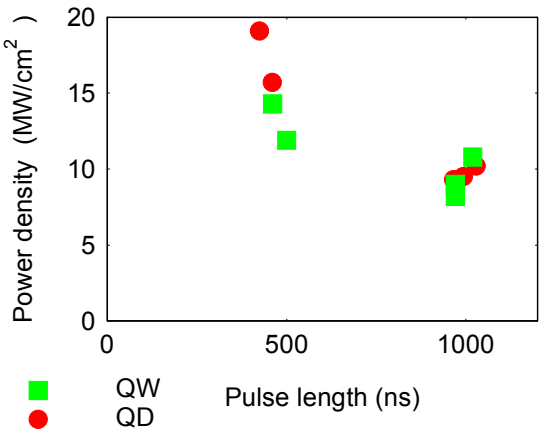

Figure 5 COMD power density limit for several different QW and QD structures including different spot sizes, pulse lengths, Al fractions in the cladding layers and different width spacer layers in the QD structures.

3. FACET TEMPERATURE MEASUREMENT

3.1 Factors affecting the facet temperature

In order to help explain the difference in behaviour between QD and QW at short pulse length in terms of physical processes we investigated the temperature rise at the facet in both QD and QW as a function of laser power at pump currents of up to twice threshold. This is the region of most interest, because in this range it should be possible to differentiate between the effects of non-radiative recombination of injected carriers, which saturates at threshold [14] and reabsorption of laser radiation leading to generation and non-radiative recombination of carriers at the facet, accompanied by heating,[15], which starts at threshold and increases with laser power. This should confirm whether the use of QD active regions gives a significant advantage.

Various direct and indirect methods exist to obtain the facet temperature such as micro-Raman spectroscopy, thermoreflectance and infra-red thermography which have different capabilities in terms of probe depth and spatial and temporal resolution. With some methods the probe used actually affects the operation of the device, for example the laser used in micro-Raman can cause surface heating. Examination of the spontaneous emission from the facet does not interfere with the operation of the device.

The spontaneous emission from a quantum well can be written [16 17] in terms of the photon energy, the absorption and the Boltzmann factor as

$$L(E) \propto \alpha(E)\ E^2 \exp\left(\frac{-E}{k_B T}\right)$$

where E is the photon energy, L(E) is the spontaneous emission, α(E) is the absorption, k_B is the Boltzmann constant and T is the electron temperature. We are assuming the electron and lattice temperature are in equilibrium.

It follows that T can be obtained [18] from a region of the spectrum where α(E) is constant, which will occur in a region where the density of states is constant: in other words away from any transitions. In practice the region used was away from the quantum well on the short wavelength side where the Boltzmann approximation is valid. The temperature can be obtained from the slope ($-1/k_BT$) of a plot of ln (L/E^2) against E which will be linear if the criteria described above are

satisfied. The absorption at this wavelength is high enough to ensure that any light emitted from the bulk interior regions of the device is absorbed and only the light from the surface layers is detected: thus the facet temperature and not the bulk temperature is obtained. Temperatures up to the melting point of GaAs or GaInP are not observed because once the critical temperature is reached COMD takes place very rapidly (less than 2.3 ms [19]) compared to the temporal resolution of the measurement.

3.2 Experimental setup for facet temperature measurement

The spontaneous emission (SE) from the region where the laser light emerges from the facet is emitted in all directions. If the sample is rotated through a large enough angle (40º) any amplified spontaneous emission and the laser light itself can be rejected. (Figure 6).

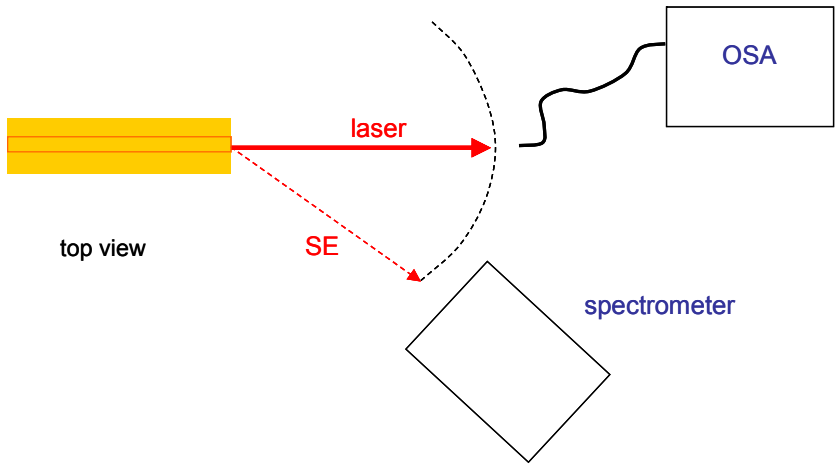

Figure 6 The experimental setup for collecting the spontaneous emission from the facet while rejecting the laser emission and amplified spontaneous emission. Any shift of the lasing wavelength was monitored using an optical spectrum analyser to check for bulk heating of the device.

To illustrate the technique the SE from the facet of a 50 µm wide oxide isolated stripe QW laser was used to obtain temperature as a function of pump current (up to 30x $_{Ith}$). (Figure 7).

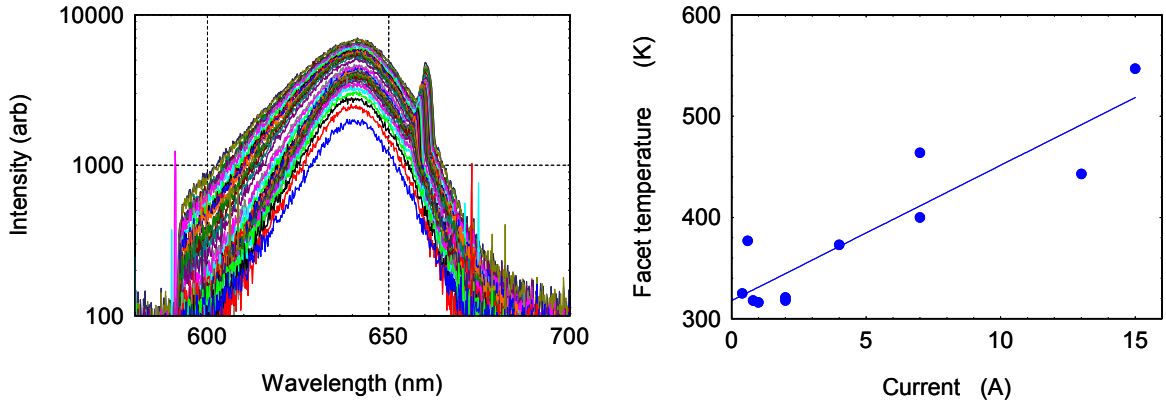

Figure 7 Log of spontaneous emission intensity as a function of wavelength for currents up to 30 x $I_{threshold}$ for a 50 µm oxide stripe QW laser. (left) A peak due to scattered lasing light can be seen at ~ 660 nm which shifts with current at these very high pumping levels indicating bulk heating. The linear region at shorter wavelength ranges was used to obtain the facet temperature (right) from the slope ($-1/k_BT$) of a plot of ln (L/E^2)

3.3 Facet temperature results

After this the SE from 5 μm wide ridge QW and QD (two of each) lasers was recorded using a grating spectrometer and CCD camera at currents (pulsed) of up to 2x threshold. The lasing spectrum was monitored using an optical spectrum analyzer (OSA) to obtain the bulk temperature of the devices. This could be subtracted from the measured facet temperature (which included both bulk and facet heating contributions.) Ridge lasers were used to ensure the temperature was measured in the region where the largest temperature increase took place. Temperatures were measured as a function of current for three different pulse lengths.

A distinct change of slope was observed at threshold for the QW lasers with a difference in the slope above threshold for different pulse lengths. (Figure 8.).

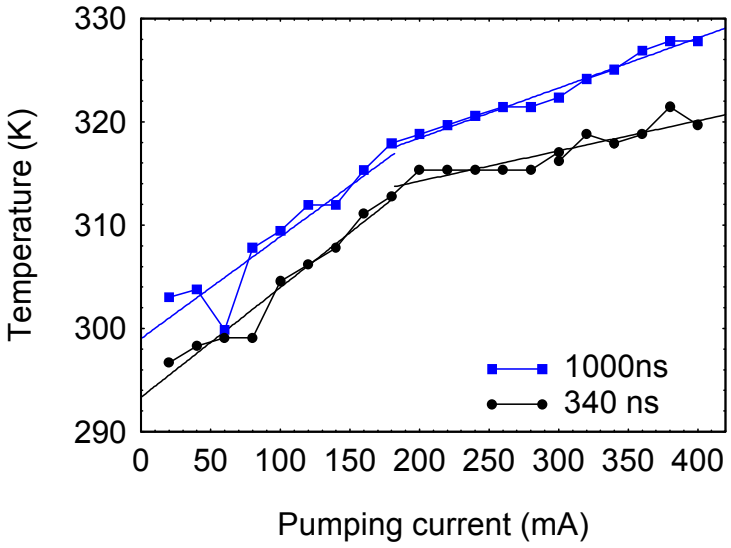

Figure 8 An example of temperature data as a function of pumping current in a QW ridge laser for two different pulse lengths. Threshold current was about 180 mA. A distinct change of slope was observed at threshold with a change in the slope above threshold for different pulse lengths.

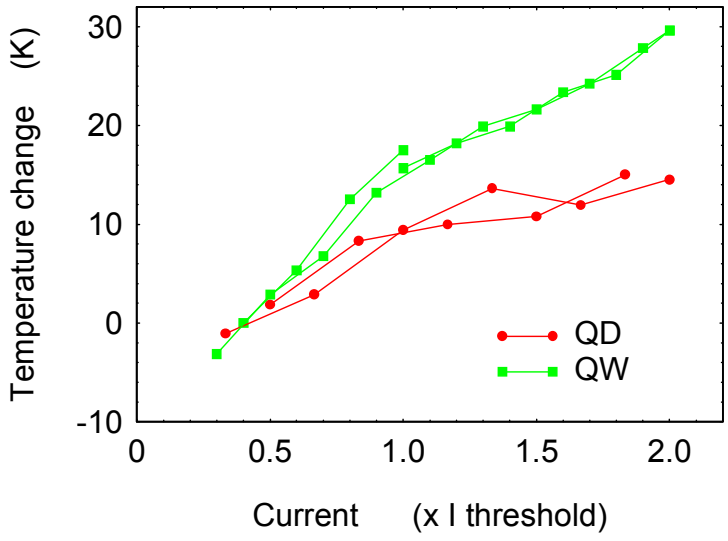

Figure 9 An example of data comparing the temperature rise in QW and QD at a pulse length of 600 ns. Currents have been normalised to $I_{threshold}$ and temperature changes referenced to the temperature at 0.4x $I_{threshold}$.

The measurements were then repeated in QD devices and a comparison made (Figure 9). In order to compare below and above threshold data for QW and QD the temperature data was normalised to multiples of $I_{threshold}$ and temperature change from $0.4xI_{threshold}$ was plotted. Lasing wavelength measurements, with the aid of separate calibration runs, were used to establish the change in bulk temperature was less than 5K but the data was not precise enough to subtract from the facet temperature data. Instead we calculated the temperature rise between 1x and 2x threshold for the QW and the QD devices. If the difference in temperature rise between QW and QD devices was greater than 5K (the maximum bulk temperature rise) it could be said that there was a difference in performance between the QW and QD devices. (Table 2)

Table 2 Facet temperature rise between 1x and 2x threshold current for QW and QD ridge devices. The differences are greater than the maximum possible bulk temperature rise indicating a difference in physical characteristics of QW and QD active regions.

pulse length	facet temp rise QW (K)	error (K)	facet temp rise QD (K)	error (K)	difference QW-QD (K)
340 ns	12.3	± 0.7	3.8	± 3.8	8.5 ±3.8
600 ns	13.8	± 0.4	5.8	± 1.8	8.0 ±1.8
1000 ns	15.2	one set	5.3	±1.6	9.9 ±1.6

4. SCANNING ELECTRON MICROSCOPY (SEM)

4.1 SEM studies of COMD

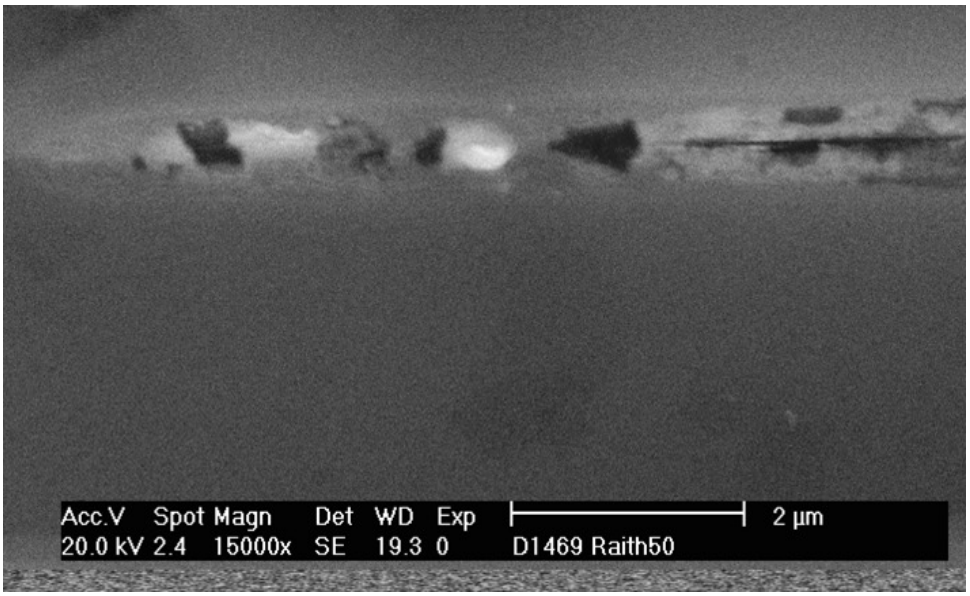

Figure 10 In SEM the damage sustained by a small part of the facet under the oxide stripe during COMD in a QW device shows more extreme damage than in a QD device, with dark and light areas and linear regions that may indicate damage at the quantum wells themselves

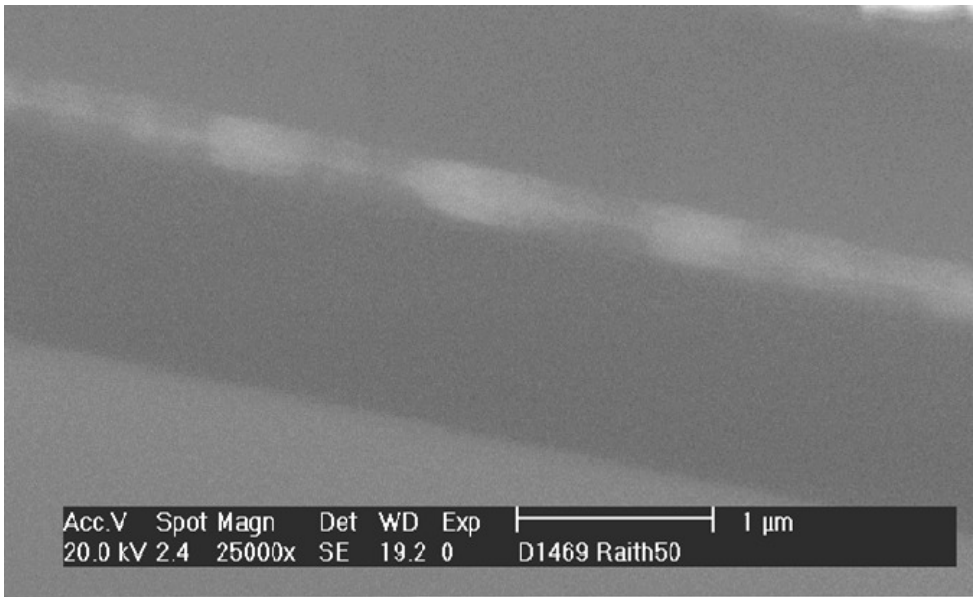

Figure 11 SEM image of the facet of a QD device that has undergone COMD showing more diffuse and less severe damage than a QW structure.

We observed a difference in the nature of the damage between QW and QD. In QW lasers (figure 10) the damage appeared to be more severe than in QD (Figure 11). In both optical microscopy and scanning electron microscope pictures (SEM) the QW structures showed much greater contrast between different spatial regions on the facet compared to QD, with regions varying from black to white through shades of grey at the quantum well area of the facet in the pumped area under the stripe. QW devices also showed the presence of ejected spheres of molten material, which were never seen in QD devices. SEM images of the facet of QD devices that had undergone COMD showed more diffuse (the focus of these images is sharp) and less severe damage with less colour contrast than a QW structure. These differences were observed for several different samples.

5. SUMMARY

Quantum dots (QD) offer significant advantages over quantum wells (QW) as the active material in high power lasers. We have determined power density values at catastrophic optical mirror damage (COMD), a key factor limiting high power laser diode performance, for various QW and QD red and NIR emitting structures in the in the AlGaInP system. The devices used were 50 µm oxide stripe lasers mounted p-side up on copper heatsinks operated pulsed. We found the COMD power density limit decreases as pulse length increases with a higher limit in QD (19.1±1.1 MW/cm^2) than in QW devices (11.9±2.8 MW/cm^2 and 14.3±0.4 MW/cm^2 for two different spot sizes) at short pulse lengths. We used the high energy Boltzmann tail of the spontaneous emission from the front facet to measure temperature rise in order to investigate the physical mechanisms (non-radiative recombination of injected carriers and reabsorption of laser light at the facet) leading to COMD and distinguish between the behaviour at COMD of QW and QD devices. Scanning electron microscopy showed a difference between the QD and QW in the appearance of the damage after COMD.

These results support the idea that quantum dots can lead to less facet heating and therefore a higher COMD power density limit for short pulse operation. They do not explain the similar behaviour seen in figure 5 for QW and QD devices at longer pulse lengths. We assume that conduction of heat away from the facet becomes more important at longer pulse length which may be due to the packaging or the particular structures that we have used. Further work is necessary to confirm these assumptions and to establish whether quantum dots can produce advantageous behaviour under cw operation.

Our study shows the COMD limit is higher for quantum dot than quantum well samples and demonstrates progress in the achievement of high powers in a quantum dot structure.

[1] Charamisinau, I., Happawana, G., Evans, G.A., Kirk, J.B., Bour, D.P., Rosen, A., and Hsi, R.A.: "High-power semiconductor red laser arrays for use in photodynamic therapy", IEEE J. Sel. Top. Quantum Electron 11(4), 881–891 (2005)
[2] Bou Sanayeh, M., Jaeger, A., Schmid, W., Tautz, S., Brick, P., Streubel, K., and Bacher, G., "Investigation of dark line defects induced by catastrophic optical damage in broad-area AlGaInP laser diodes" Appl. Phys. Lett. **89** 101111 (2006)
[3] Henry, C. H., Petroff, P. M., Logan, R. A. and Merritt, F. R., " Catastrophic Damage of $Al_xGa_{1-x}As$ double-heterostructure laser material", J. Appl. Phys. **50** (4), 3721-3732 (1979)
[4] Chen, G., and Tien, C. L., "Facet heating of quantum well lasers", J. Appl. Phys. **74** (4), 2167-2174 (1993)
[5] Tang, W. C., Rosen, H. J., Vettiger, P. and Webb, J. D., "Raman microprobe study of the time development of AlGaAs single quantum well laser facet temperature on route to catastrophic breakdown", Appl . Phys. Lett. **58** (6) 557-559 (1991)
[6] Lambert, R. W., Ayling, T., Hendry, A. F., Carson, J. M., Barrow, D. A., McHendry, S., Scott, C. J., McKee, A. and Meredith, W., "Facet Passivation Processes for the Improvement of Al-Containing Semiconductor Laser Diodes", J. Lightwave Tech., **24** (2) 956-961 (2006)
[7] Moore, S. A., O'Faolain, L., Cataluna, M. A., Flynn, M. B., Kotlyar, M. V. and Krauss, T. F., "Reduced Surface Sidewall Recombination and Diffusion in Quantum-Dot Lasers", IEEE Phot. Tech. Lett., **18**, (17), 1861-1863 (2006)
[8] Smowton, P. M., Pearce. E. J., Schneider, H. C., Chow, W. W. and Hopkinson, M., "Filamentation and linewidth enhancement factor in InGaAs quantum dot lasers", Appl. Phys. Lett. **81**(17) 3251-3253 (2002)
[9] Ribbat, Ch., Sellin, R. L., Kaiander, I., Hopfer, F., Ledentsov, N. N., Bimberg, D., Kovsh, A. R., Ustinov, V. M., Zhukov, A. E. and Maximov, M. V., "Complete suppression of filamentation and superior beam quality in quantum-dot lasers", Appl. Phys. Lett **82** (6) 952-954 (2003)
[10] Elliott, S. N., Smowton, P. M. and Berry, G., "Optimisation of high power AlGaInP laser diodes for optical storage applications",. Optoelectronics, IEE Proceedings, **153** (6), 321 – 325 (2006)
[11] Fujii, H., Ueno, Y. and Endo, K., "Effect of thermal resistivity on the catastrophic optical damage power density of AlGaInP laser diodes" , Appl. Phys. Lett. **62** (17), 2114-2115 (1993)
[12] Tang, W. C., Rosen, H. J., Vettiger, P. and Webb, D. J., "Raman microprobe study of the time development of AlGaAs single quantum well laser facet temperature on route to catastrophic breakdown" Appl. Phys. Lett. **58** (6) 557-559 (1991)
[13] Carslaw, H. S. and Jaeger J. C., "Conduction of heat in solids", 2nd Ed. (Oxford U. P., London, 1959)
[14] Malyarchuk, V., Tomm, J. W., Talalaev, V. and Lienau, Ch. "Nanoscopic measurements of surface recombination velocity and diffusion length in a semiconductor quantum well", Appl. Phys. Lett **81** (2) 346-348 (2002)
[15] Ziegler, M., Talalaev, V., Tomm, J. W., Elsaesser, T., Ressel, P., Sumpf, B. and Erbert, G. "Surface recombination and facet heating in high-power diode lasers", Appl. Phys. Lett. **92** 203506 (2008)
[16] Henry C. H., Logan, R. A. and Merritt, F. R., "Measurement of gain and absorption spectra in Al GaAs buried heterostructure lasers", J. Appl. Phys. **51** (6), 3042-3050 (1980)
[17] Blood, P., Kucharska, A. I., Jacobs, J. P. and Griffiths, K., "Measurement and calculation of spontaneous recombination current and optical gain in GaAs-AlGaAs quantum-well structures", J. Appl. Phys. **70** (3) 1144-1156 (1991)
[18] Sweeney, S. J., Lyons, L. J., Adams, A. R. and Lock, D. A., " Direct Measurement of Facet Temperature up to Melting Point and COD in High-Power 980-nm Semiconductor Diode Lasers", IEEE J. S. T. Q. E. **9** (5) 1325-1332 (2003)
[19] Ziegler, M., Tomm, J. W., Elsaesser, T., Matthiessen, C., Bou Sanayeh., M. and Brick, P., "Real-time thermal imaging of catastrophic optical damage in red-emitting high-power diode lasers", Appl. Phys. Lett. **92** 103514 (2008)